Use of dyadic Green's function for RCS estimation of large targets

Erwan Gillion, Erwan Rochefort, Jacques Claverie, Christian Brousseau

Use of dyadic Green's function for RCS estimation of large targets

E. Gillion[1,2], E. Rochefort[2], J. Claverie[1,3], C. Brousseau[1]

[1] IETR – Institut d'Electronique et de Télécommunications de Rennes, UMR CNRS 6164, Université de Rennes 1, Rennes, France

[2] CMN – Constructions Mécaniques de Normandie, Cherbourg, France

[3] CREC St-Cyr, LESTP, Guer, France

***Abstract*—This paper presents a new method to estimate the Radar Cross Section (RCS) of a large object in its environment. This estimation method is based on dyadic Green's function method which includes near-field issues. Simulations results are discussed using canonical targets in a frequency band between 1 to 20 GHz. The RCS figures taking into account the volumetric representation of the target, the near-field region and maritime environment, are presented here.**

***Index Terms*—Radar Cross Section, Green's function, near-field**

I. INTRODUCTION

In the remote sensing domain, one common application in naval electronic warfare is the radar detection of ships based on the RCS (Radar Cross Section) measurement. The RCS value of a ship can be regarded as its identity card. In the past, ship manufacturers measured the RCS value after the ship was built to estimate its stealthy behavior. However, this method was too expensive and not efficient for ship manufacturers. Nowadays, it is more common to predict the RCS value of a ship before its building to comply with the specifications. This method grants the possibility to modify the design of the ship to increase its stealthy behavior during the conception phase.

Over the past decades, numerous methods have been developed to predict the RCS value of objects, like PO (Physical Optics), PTD (Physical Theory of Diffraction) or MoM (Method of Moments) [1], [2]. Also, estimation is done considering the free-space approximation. However, when a large object is surrounded by inhomogeneous medium, usual methods do not reflect the reality [3]. Another approach is to derivate de the dyadic Green's function to estimate the RCS value, taking into account the volumetric representation of the target, the near-field region and the whole environment parameters.

This paper is organized as follows. In Section II, the classical RCS estimation is presented for a simple scatterer over the sea and taking into account the evaporation duct effect. Section III presents the limitation of the classical method applied to a large target and a solution to this problem is proposed. Finally, a validation of the proposed method is realized in Section IV, showing the importance of the near-field consideration in the RCS estimation.

II. RCS ESTIMATION

A. RCS definition

The formal RCS equation σ_0 is defined in a lossless medium by considering the target located at an infinite distance from the radar [1]:

$$\sigma_0 = \lim_{R \to \infty} 4\pi R^2 \frac{\left|\mathbf{E}_s\right|^2}{\left|\mathbf{E}_i\right|^2}. \quad (1)$$

where $\mathbf{E}_i$ and $\mathbf{E}_S$ are respectively the incident and the scattered fields, and R, the distance between the radar and the target. In real configurations, targets RCS are estimated at distances considerably less than infinity. Generally, the estimation distance R is assumed close to infinity if its value is great enough to consider propagation for both incident and scattered fields in far-field condition. In addition, the propagation medium is not lossless in real cases.

In a complex environment, the apparent RCS figure σ_{app} is usually used [3]. By assuming far-field propagation between the radar and the target, an approximated method to estimate the apparent RCS σ_{app} is given by multiplying the free-space RCS σ_0, by the two-way propagation factor which characterizes the environment:

$$\sigma_{app} = \sigma_0 . F^4 . \quad (2)$$

where the one-way propagation factor F^2 is given by:

$$F^2 = \left|\mathbf{E}_{tot}\right|^2 / \left|\mathbf{E}_0\right|^2 . \quad (3)$$

with $\mathbf{E}_{tot}$, the total field at the target location, and $\mathbf{E}_0$, the field under free-space condition at the same location.

It is important to notice that, by definition, the formal RCS σ_0 only depends to the target characteristics. For this reason, it is common to assume that the target is represented by a simple scatterer in the apparent RCS calculation where the scatterer RCS diagram corresponds to the formal RCS diagram of the target. This implies that variations of the apparent RCS value σ_{app} of a target are directly proportional to the propagation factor variations when using (2).

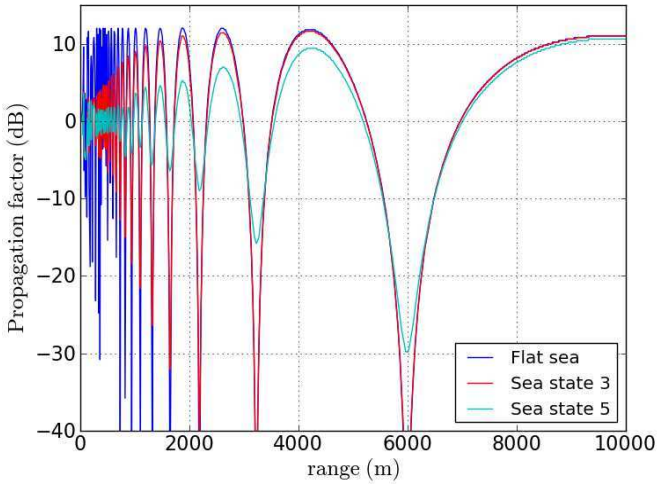

Figure 1. Impact of the sea roughness on the two-way propagation factor as a function of range, at 5 GHz and for different Douglas sea states. Radar and scatterer are located at a same heigth (10 m). Results are compared to the standard case (flat sea and no duct).

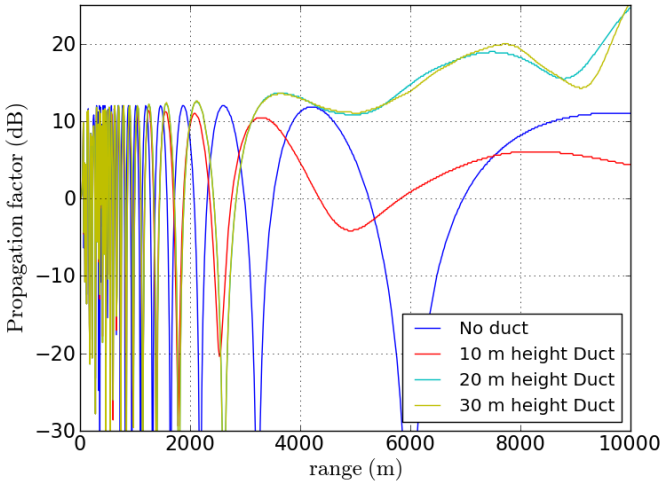

Figure 2. Impact of the evaporation duct on the two-way propagation factor as a function of range, at 5 GHz and for different duct heights. Radar and scatterer are located at the same heigth (10 m). Results are compared to the standard case (flat sea and no duct).

B. Medium influence

In radio waves propagation, especially over the sea surface, medium parameters have a strong impact on the propagation factor value. The most significant effects are the sea roughness and the evaporation duct [3]. Sea roughness effect describes the influence of sea waves on the diffusion of EM waves, and evaporation duct effects can trap EM waves within a surface-based waveguide.

Sea roughness effect modifies propagation factor value proportionally to the sea state, as shown in Fig 1. The smoothing of curves corresponds to the multipath and the shadowing effects due to sea waves. We can notice that for a sea state lower than 3 (Douglas sea scale), results are similar to the standard case (no duct, flat sea) after 1 km. For sea state upper than 3, the observed propagation factor value is lower and merges with the standard case curve farther.

Furthermore, evaporation duct effect increases or decreases the propagation factor value. The impact of the ducting effects on the propagation factor is show in Fig. 2 and compared to the standard case (no duct, flat sea). As shown in this figure, the impact of this effect on the propagation factor value depends strongly to the radar range, the target location and the evaporation duct properties.

TABLE I. DESCRIPTION OF THE IMPACT OF THE SEA ROUGHNESS AND THE EVAPORATION DUCT ON THE PROPAGATION FACTOR.

Sea states	***Description***	***Sea roughness***	***Evaporation duct***
0	Flat sea	Ø	++
1 – 2	Small sea waves	–	++
3 – 4	Moderate sea waves	+	+
5 – 6	High sea waves	++	–
> 6	Very high sea waves	++	–

++. Very strong impact, +. Strong impact, –. Low impact, Ø. Inexistent

Consequently, evaporation duct and rough sea must be considered together in RCS prediction models. These two effects can work in the same way (decrease RCS) or in the opposite ways. Table 1 roughly summarizes interaction between sea roughness and evaporation duct for different Douglas sea scale.

III. RCS OF A LARGE TARGET

In this section, a large target is considered. As shown on Fig. 1 to 3, for a standard case (no duct, flat sea), the position of the scatterer already has an impact on its RCS. According to Fig. 3, the observed two-way propagation factor values vary from +12 dB to less than -30 dB depending to the scatterer height. In the case of a large target, its height will weight the propagation factor value. Thus, the target can no longer be described by a simple scatterer in (2) but by a set of scatterers or by meshed surfaces.

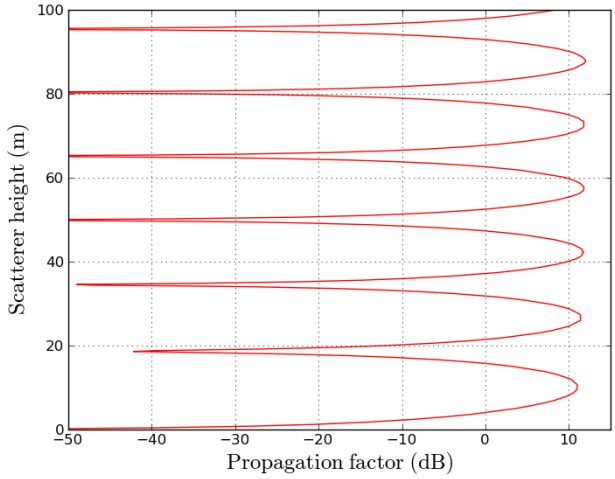

Figure 3. Two-way propagation factor over the sea as a function of scatterer height in a standard case (no duct, no roughness), observed at 10 km from the radar for a frequency of 10 GHz. The radar is located 10 m above sea level.

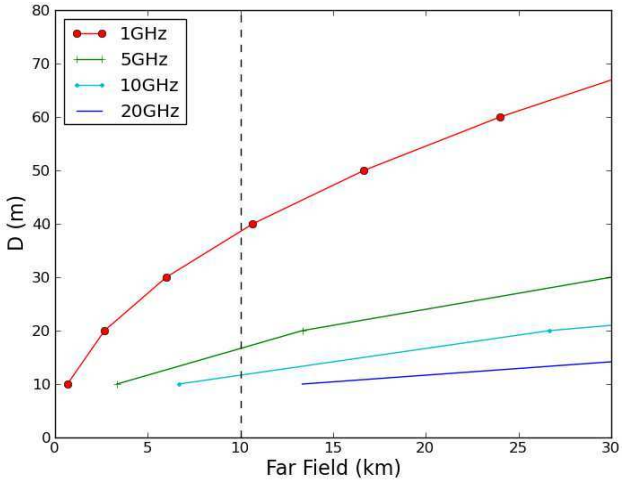

Figure 4. Minimum far-field distance as a function of the target dimensions D, for different frequencies between 1 GHz and 20 GHz.

Additionally, as the volumetric behavior of the target is taken into account, the far-field assumption considered in (2) must be verified by using the Fraunhofer's far-field criterion in forward and backward propagation:

$$d > 2.\mathrm{D}^2/\lambda\,. \tag{4}$$

where d is the minimum far-field distance, D is the largest dimension of the target and λ is the wavelength.

Radar antennas are specially designed to minimize the size of the near-field region. Generally, the far-field region starts relatively close to the antenna in comparison to the common radar range. According to this, the far-field propagation assumption remains true in the case of the forward propagation (from the radar to the target).

For the backward propagation, it is known that any target illuminated by an electromagnetic wave will act like an antenna. In naval applications, targets dimensions (i.e. length or height) are generally greater than 10 m and the common RCS measurement range for a ship is close to 10 km.

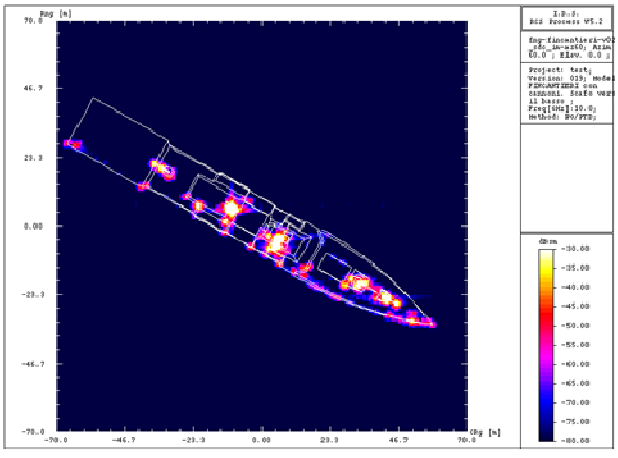

Figure 5. ISAR figure of a ship to illustrate hotspots phenomenon.

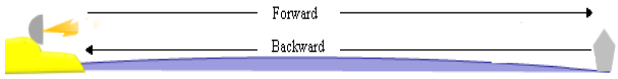

Figure 6. Illustration of the forward and backward propagation.

By considering a 40×15 m-sized naval target, the minimum Fraunhofer distance d is equal to 107 km at 10 GHz (Fig. 4) while the radar line-of-sight for an antenna located 25 m above the sea level is equal to 40 km in standard propagation conditions. Here, the far-field assumption is invalidated in the case of the backward propagation (i.e. from the target to the radar). Thus, backward propagation shall take into account near-field issues by a perfect description of the target's volumetric characteristics. A hotspots representation could refer to the latter (Fig. 5).

These simple remarks contradict the rule which match the forward propagation factor to the backward one, which is the far-field assumption. A subdivision of propagation factor, as illustrated on Fig 6, should always be defined if the backward or forward propagation do not respect the Fraunhofer's criterion.

Thus, the RCS estimation of large targets over the sea, like military vessels, must take into account the near-field consideration. This implies that the apparent RCS σ_{app} must be specified by a more suitable expression, derived from the exact RCS formula including near-field consideration [4]:

$$\sigma_{app} \approx 4\pi R^4 Z \frac{\left|\mathbf{E}_\mathrm{S} \times \mathbf{H}_\mathrm{S}^*\right|}{\left|V_\mathrm{i}\right|^2}\,. \tag{5}$$

where V_i is the magnitude of the transmitted EM field, Z, the medium impedance, and $\mathbf{H}_\mathrm{S}^*$, the conjugate of the scattered magnetic field.

In this case, a solution to determine the scattered field $\boldsymbol{E}_\mathrm{S}$ is the use of dyadic Green's function, developed from scalar Green's function [5]. This choice was based on the following criteria:

- This is an exact method which includes near-field and far-field considerations.
- This function is applicable in the 2D and 3D configurations.

The scattered field computed by this method can be formulated as follows [6]:

$$\mathbf{E}_\mathrm{S}(\mathrm{P}) = \mathrm{j}\omega\mu_0 \iiint_\mathrm{V} \overline{\overline{\Gamma}}(M,P)\mathbf{J}_\mathrm{S}(M)\mathrm{dV}(M)\,. \tag{6}$$

where $\omega = 2\pi f$ is the pulsation of the EM field, μ_0, the permeability of vacuum, $\boldsymbol{J}_s$, the surface current density on the target surface, Γ, the dyadic Green's function [6], M, a point located on the source, and P, the location of the receiver. The RCS of a large target is then estimated by applying (6) in (5).

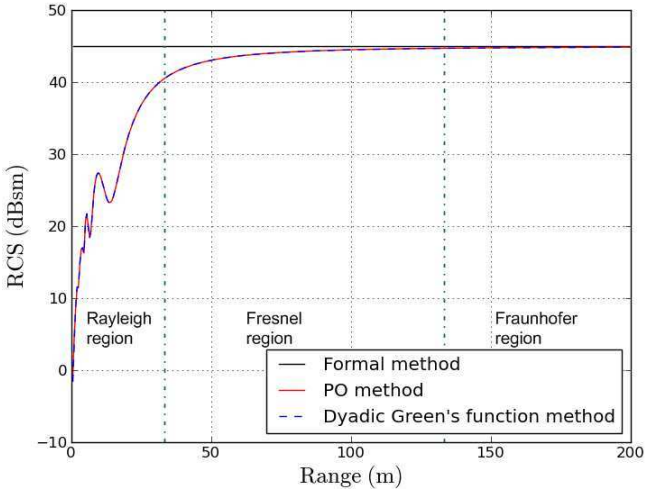

Figure 7. Free-space monostatic RCS as a function of range, for a 1×1 m PEC plate, for normal incidence at 15 GHz.

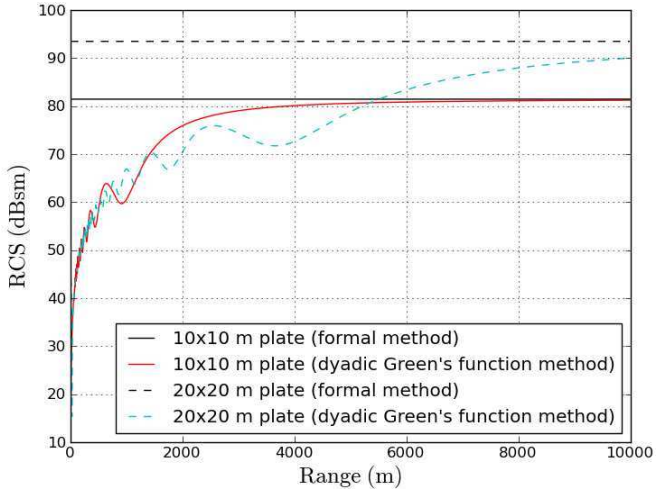

Figure 8. Free-space monostatic RCS as a function of range for a 10×10 m and 20×20 m square plates, for normal incidence at 10 GHz.

IV. SIMULATION RESULTS

To evaluate the dyadic Green's function method in RCS estimation, the free-space RCS figure computed by this method is compared to the free-space RCS figure estimated from the formal method given by (1) and from the PO method [4]. Thus, the free-space monostatic RCS of a 1×1m perfectly electrical conductor (PEC) plate at normal incidence is calculated at a frequency of 15 GHz (Fig. 7). A good agreement is observed between the results from the dyadic Green's function method and from the PO method. Moreover, by comparing these two methods to the formal one, some important variations of the RCS value are observed on the first 60 m. This implies that a near-field RCS is observed even if the near-field zone is located close to the radar due to the small sizes of the plate.

To illustrate this phenomenon, simulations on larger targets are needed. Thus, free-space monostatic RCS of a 10×10 m and 20×20 m PEC flat plates are computed at the X-band frequency of 10 GHz (Fig 8). Results are compared to the formal RCS value computed by (1). As expected, the near-field behaviour of the RCS is observed for more significant distances as the sizes of the plate increase. Indeed, the RCS of the 20×20 m plate is still in the Rayleigh region at 10 km.

Afterward, for a more realistic approach the sea effect is implemented in the dyadic Green's function method. The RCS of a 10×10 m PEC plate located 10 m above a flat sea is then computed at 10 GHz (Fig. 9). As expected, important differences between the free-space formal method (1) and the approximated method (2) or the dyadic Green's function method are observed. Moreover, the approximated method and the dyadic Green's function method results are equivalent when the size of the target is small compared to the radar-target distance (Fig. 9 and Fig. 10). It is also interesting to point out that the apparent RCS figures computed by the dyadic Green's function over the sea meets the formal one for some ranges.

The last remark is already observed on the RCS figure of a 20×20 m PEC plate located 10 m above a flat sea at 10 GHz (Fig. 10). In this case, the dyadic Green's function method figure is close to the formal one from 9 to 35 km. It is however important to specify that the RCS values are computed for targets in vacuum, standing over the sea and by assuming a flat earth. Thus, the ranges where these two RCS prediction methods correspond could differ in a more realistic approach by taking into account atmosphere and earth curvature.

Finally, to take into account the impact of sea roughness in RCS estimation, the Miller & Brown coefficient [7] is implemented into the dyadic Green's function. The RCS figures of a 10×10 m and a 20×20 m sized PEC flat plate located 10 m above a rough sea are computed at 10 GHz and for different Douglas sea states (respectively Fig. 11 and Fig. 12). As expected, a smoothing of curves is observed when the sea state increases. Moreover, the apparent RCS figure becomes close to the free-space RCS figure for strong sea states.

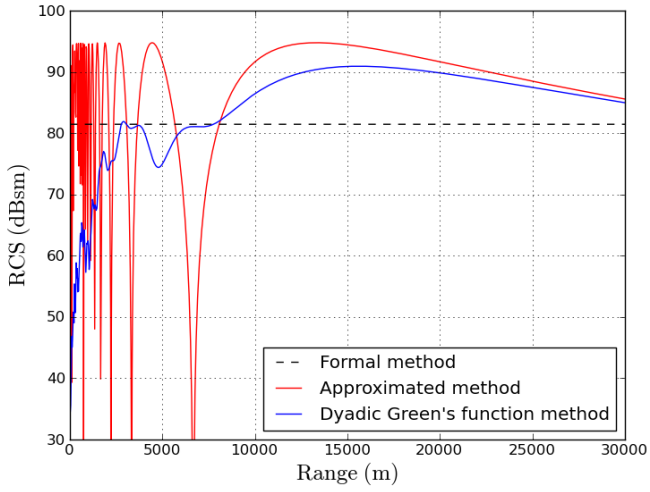

Figure 9. Monostatic RCS as a function of range for a 10×10 m PEC plate at normal incidence centered at 10 m above a flat sea at 10 GHz.

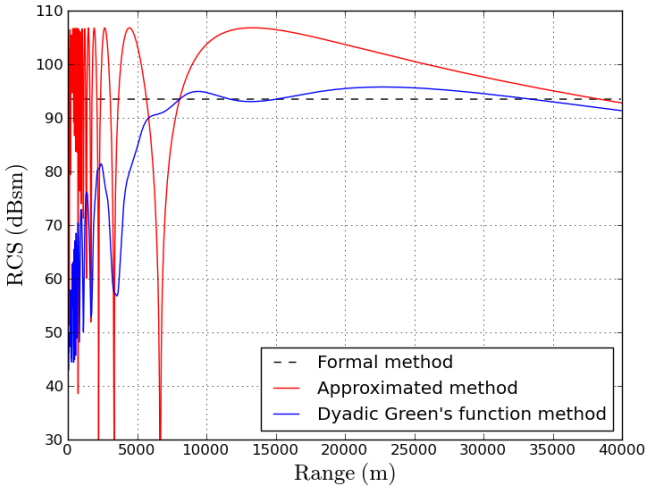

Figure 10. Monostatic RCS as a function of range for a 10×10 m PEC plate centered 10 m above a flat sea for normal incidence at 10 GHz.

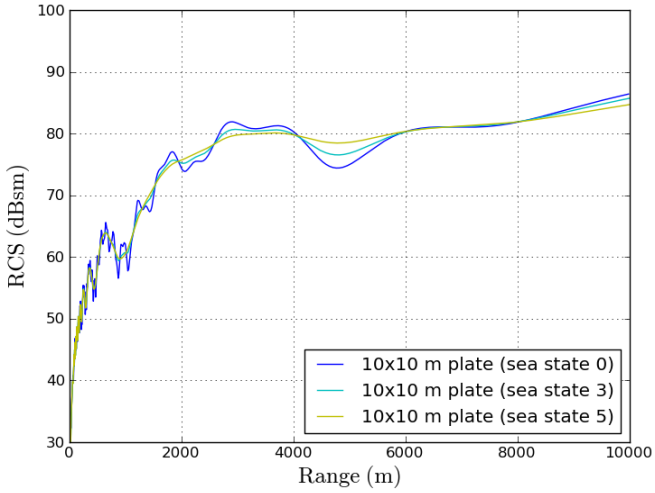

Figure 11. Monostatic RCS as a function of range for a 10×10 m square plate centered 10 m above a rough sea, for normal incidence at 10 GHz. Comparison of RCS values for different Douglas sea states.

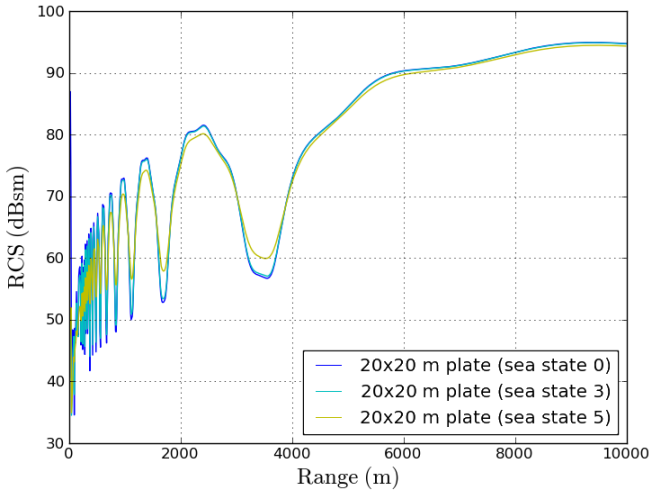

Figure 12. Monostatic RCS as a function of range for a 20×20 m square plate centered 10 m above a rough sea, for normal incidence at 10 GHz. Comparison of RCS values for different Douglas sea states.

V. CONCLUSION

In this paper, RCS estimation of large objects in naval environment is investigated. It is shown that usual methods developed for complex environments met some important lacks of precision as the target dimensions increase. Indeed, presented results show that the backscattered field computation in RCS estimation of large targets must takes into account both near-field and far-field issues. In these conditions, a dyadic Green's function method is proposed and validated with results obtained from canonical PEC plate targets in vacuum, standing over a rough surface. However, a final RCS representation taking into account near-field issues and atmospheric effects have not been implemented yet in our dyadic Green's function model.

In this way, our future work in RCS prediction will lead to include atmospheric parameters in dyadic Green's function. Starting from this method, a complete validation by real data shall be made.

REFERENCES

[1] E. F. Knott, J. F. Shaffer and M. T. Tuley, "Radar Cross Section", 1st ed., Artech House, New York, USA, 1985.

[2] M. Skolnik, "Radar handbook", 2nd ed., McGraw-Hill, New York, USA, 1990

[3] J. Claverie and Y. Hurtaud, "Variation of the apparent RCS of maritime targets due to ducting effects", AP2000 – IEEE Millenium Conference on Antennas and propagation, Davos, Switzerland, 9-14 April 200.

[4] P. Pouliguen, R. Hermon, C. Bourlier, J. F. Damiens, and J. Saillard, "Analytical formulae for Radar Cross Section of flat plates in near-field and normal incidence," Progress In Electromagnetics Research B, vol. 9, pp. 263–279, 2008.

[5] D.G. Duffy, "Green's functions with applications", Chapman&Hall, CRC, 2001.

[6] C.T. Tai, "Dyadic Green's function in Electromagnetic Theory", 2nd ed., IEEE Press, 1993.

[7] A.R. Miller, "New derivation for the rough surface reflection coefficient and for the distribution of sea-wave elevations", IEEE Proc., Vol. 131, No. 2, April 1984.